# Integrated System for the Complete Segmentation of the Common Carotid Artery Bifurcation in Ultrasound Images

Christos Loizou, Takis Kasparis, Christina Spyrou, Marios Pantziaris



# Integrated System for the Complete Segmentation of the Common Carotid Artery Bifurcation in Ultrasound Images

Christos P. Loizou[1*], Takis Kasparis[2], Christina Spyrou[2], and Marios Pantziaris[3]

[1] Department of Computer Science, Intercollege, P. O. Box 51604, CY-3507, Limassol, Cyprus {panloicy@logosnet.cy.net} [2]Cyprus University of Technology, Dept. of Electical, Computer Engineering and Informatics, Limassol, Cyprus {takis.kasparis@cut.ac.cy} [3]Cyprus Institute of Neurology and Genetics, Nicosia, Cyprus {pantzari@cing.ac.cy}

**Abstract.** The complete segmentation of the common carotid artery (CCA) bifurcation in ultrasound images is important for the evaluation of atherosclerosis disease and the quantification of the risk of stroke. This requires the extraction of the intima-media complex (IMC), the delineation of the lumen the atherosclerotic carotid plaque and measurement of the artery stenosis. The current research proposes an automated segmentation system for the complete segmentation of the CCA bifurcation in ultrasound images, which is based on snakes. The algorithm was evaluated on 20 longitudinal ultrasound images of the CCA bifurcation with manual segmentations available from a neurovascular expert. The manual mean±SD measurements were for the IMT: (0.96±0.22) mm, lumen diameter: (5.59±0.84) mm and ICA origin stenosis (48.1±11.52) %, while the automated measurements were for the IMT: (0.93±0.22) mm, lumen diameter: (5.77±0.99) mm and ICA stenosis (51.05±14.51) % respectively. We found no significant differences between all manual and the automated segmentation measurements.

***Keywords:*** Intima-media thickness; lumen diameter; atherosclerotic plaque, carotid segmentation; ultrasound image; carotid artery.

## 1 Introduction

Atherosclerosis of the carotid artery is a pathological process mainly affecting the common carotid artery (CCA) bifurcation and is one of the major clinical manifestations leading to cardiovascular disease (CVD). It causes thickening of the artery walls, which affects blood flow, and may develop atherosclerotic carotid plaques, which causes stenosis in the artery lumen, thus affecting the normal blood flow [1]. Atherosclerosis can result to heart attack, and stroke [1].

Carotid intima-media-thickness (IMT) is a measurement of the thickness of the innermost two layers of the arterial walls and provides the distance between the lumen-intima and the media-adventitia. The IMT can be observed and measured as the double line pattern on both walls of the longitudinal images of the CCA [2], [3] (see also Fig. 1) and it is well accepted as a validated surrogate marker for

atherosclerotic disease [1]. Furthermore, the arterial stenosis is a significant marker of atherosclerosis and can be evaluated through the segmentation of atherosclerotic carotid plaques [4].

There are a number of segmentation methods proposed in the literature for the segmentation of the IMT, [2], [3], carotid diameter [4], [5], and the atherosclerotic carotid plaque [6], from ultrasound images of the CCA bifurcation, but there are no other studies reported where a complete segmentation of the CCA artery bifurcation has been attempted. More specifically, in [2] a review of different automated or semi-automated techniques for the segmentation of the IMT was reported, while in [3] a snakes based system for the segmentation of IMT in ultrasound images of the CCA was proposed. In [7], the system proposed in [3] was further extended for segmenting the intima layer and the media layer in ultrasound images of the CCA were additionally speckle reduction [8], [9] was applied in the image as a preprocessing step. Different carotid artery diameter indices were proposed in [4] and [5] where the lumen diameter was segmented and measured. Finally, in [6] a snakes based segmentation system was proposed for the segmentation of the atherosclerotic carotid plaque from ultrasound images of the CCA. The system requires the blood flow image, from which an initial contour estimation for the carotid plaque borders is estimated, which is then used as an input to the snake's segmentation algorithm.

All above integrated systems were proposed either for the segmentation of the IMC, lumen diameter or atherosclerotic plaque and there is no other system proposed earlier in the literature for integrating all above segmentation techniques in one software application. It is therefore desirable for the clinical expert to be able to use an integrated segmentation system, in which all the above aforementioned techniques could be integrated together in order to evaluate in a more precise and objective way the risk of stroke in asymptomatic and symptomatic subjects at risk of stroke .

In this study, our objective was to develop and evaluate an automated integrated segmentation system based on snakes, for segmenting the IMC, the atherosclerotic carotid plaque and the lumen diameter in longitudinal ultrasound images of the CCA bifurcation.

The segmentation system proposed in this study was evaluated on 20 ultrasound images acquired from symptomatic subjects and were compared with the manual delineations made by a neurovascular expert. We found no statistical significant differences between the manual and the automated segmentation measurements. The findings of this study indicate that the proposed system may also be effectively applied in the clinical praxis.

The following section presents the materials and methods used in this study, whereas in section 3, we present our results. Sections 4 and 5 give the discussion, and the concluding remarks respectively.

## 2 Materials & Methods

### 2.1 Recording of ultrasound images

A total of 20 B-mode longitudinal ultrasound images of the CCA bifurcation, with atherosclerotic plaques, were recorded (task carried out by co-author M. Pantziaris). The images display the vascular wall as a regular pattern (see Fig. 1a) that correlates with anatomical layers. The images were collected from symptomatic subjects, which have already developed clinical symptoms, such as a stroke or a transient ischemic attack at a mean±SD age of 48±10.47 years. The images were acquired by the ATL HDI-5000 ultrasound scanner (Advanced Technology Laboratories, Seattle, USA) [10] with a resolution of 768x576 pixels with 256 gray levels. We use bicubic spline interpolation to resize all images to a standard pixel density of 16.66 pixels/mm (with a resulting pixel width of 0.06 mm). For the recordings, a linear probe (L 7-4) at a recording frequency of 4-7 MHz was used. Assuming a sound velocity propagation of 1550 m/s and 1 cycle per pulse, we thus have an effective spatial pulse width of 0.22 mm with an axial system resolution of 0.11 mm [10]. Consent from each subject was obtained according to the instructions of the local ethics committee.

### 2.2 Ultrasound image normalization

Brightness adjustments of ultrasound images were carried out in this study based on the method introduced in [11], which improves image compatibility by reducing the variability introduced by different gain settings, different operators, different equipment, and facilitates ultrasound tissue comparability. Algebraic (linear) scaling of the images were manually performed by linearly adjusting the image so that the median gray level value of the blood was 0-5, and the median gray level of the adventitia (artery wall) was 180-190 [11]. The scale of the gray level of the images ranged from 0-255. Thus the brightness of all pixels in the image was readjusted according to the linear scale defined by selecting the two reference regions. Further details of the proposed normalization method can be found in [6]-[9].

### 2.3 Manual measurements

A neurovascular expert (task carried out by co-author M. Pantziaris) manually delineated (in a blinded manner, both with respect to identifying the subject and delineating the image by using the mouse) the IMC, the atherosclerotic plaque and the lumen diameter [3], on all longitudinal ultrasound images of the CCA bifurcation after image normalization (see subsection 2.2) and speckle reduction filtering (see subsection 2.4). The IMT was measured by selecting 10 to 20 consecutive points for the intima and the adventitia layers, while by selecting 20 to 30 consecutive points for the near and far wall of the CCA respectively. The atherosclerotic plaque was measured by selecting 20-30 consecutive points forming a closed contour, while the lumen was measured by selecting the adventitia at the near wall of the CCA and the origin of the ICA. The manual delineations were performed using a system

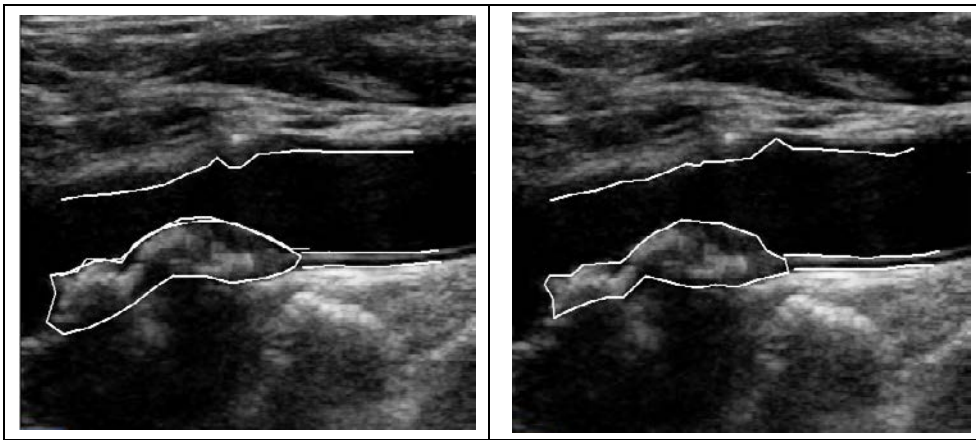

(a) Manual CCA full segmentation | (b) Automated CCA full segmentation

Figure 1. a) Manual full CCA segmentation ($IMT_{mean}$=0.73 mm, $IMT_{max}$=0.85 mm, $IMT_{min}$=0.55 mm, $IMT_{median}$=0.66 mm, $D_{mean}$=5.51 mm, $D_{max}$=6.80 mm, $D_{min}$=3.31 mm, $D_{median}$=5.78 mm), and b) automated full CCA segmentation ($IMT_{mean}$=0.72 mm, $IMT_{max}$=0.83 mm, $IMT_{min}$=0.51 mm, $IMT_{median}$=0.67 mm, $D_{mean}$=5.65 mm, $D_{max}$=6.92 mm, $D_{min}$=3.45 mm, $D_{median}$=5.75 mm) from a symptomatic subject at risk of stroke the age of 53.

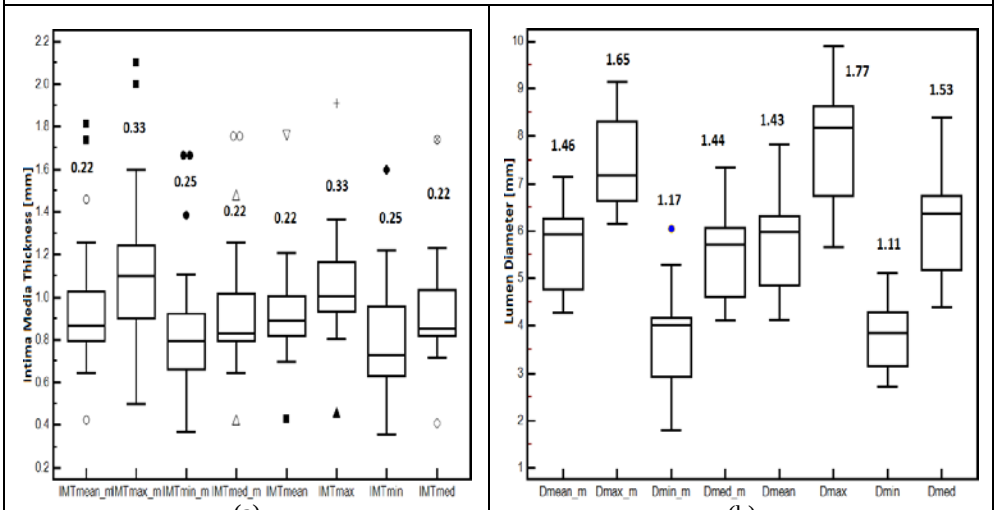


(a) (b)

Figure 2. Box plots for the mean, maximum, minimum and median segmentation measurements of the CCA for the: (a) IMT, and (b) Lumen diameter (D). From left to right, we present the mean manual and automated IMT (IMT_m, IMT), and D (D_m, D) for all 20 patients investigated. Inter-quartile rage values are shown above the box plots. Straight lines connect the nearest observations with 1.5 of the inter-quartile range (IQR) of the lower and upper quartiles. Unfilled rectangles indicate possible outliers with values beyond the ends of the 1.5xIQR.

implemented in Matlab (Math Works, Natick, MA) from our group. The

measurements were performed on the far wall between 2 cm proximal to the bifurcation of the CCA [11] ending at a point 2.0 cm distal to the bifurcation of the CCA [12]. The IMT, the atherosclerotic plaque geometrical measures, and the lumen diameter, were then calculated as the average of all the measurements. The measuring points and delineations were saved for comparison with the snake's segmentation method.

### 2.4 Speckle reduction filtering (DsFlsmv)

In this study the linear scaling filter (despeckle filter linear scaling mean variance-DsFlsmv) [13], utilizing the mean and the variance of a pixel neighborhood was used to filter the CCA ultrasound images from multiplicative noise prior the full segmentation of the CCA. The filter may be described by a weighted average calculation using sub region statistics to estimate statistical measurements over 5x5 pixel windows applied for two iterations [8], [9]. Further implementation details of the DsFlsmv despeckle filter may be found in [8].

### 2.5 Automatic IMC, lumen and plaque snakes segmentation

The IMC, lumen and plaque of the CCA were automatically segmented after image normalization and despeckle filtering (see section 2.2 and section 2.4), using an automated snake's segmentation system proposed and evaluated for the segmentation of the IMC in [3] and the plaque in [6]. The stenosis of the artery was then estimated using the Carotid Stenosis Index (CSI) [4], [12] as follows:

$$CSI = (1 - \frac{N}{D}) * 100 \quad (1)$$

with N, the lumen diameter in maximum stenosis location, and D the lumen diameter of distal CCA.

We present in Fig. 1b the automated results of the final snake contours after snake's deformation for the IMT, the carotid lumen diameter, D, and the atherosclerotic carotid plaque at the far wall of the CCA. These were automatically segmented by the proposed segmentation system. An IMT, D, and plaque initialization procedure was carried out for positioning the initial snake contour as close as possible to the areas of interest, which is described in [3], [6], [7].

The Williams & Shah snake segmentation method [14], was used to deform the snake and segment the IMC, D, and plaque borders. For the Williams & Shah snake, the strength, tension and stiffness parameters were equal to $\alpha = 0.6$, $\beta_s = 0.4$, and $\gamma_s = 2$ respectively. The extracted final snake contours (see Fig. 1b), corresponds to the adventitia and intima borders of the IMC, the carotid diameter, D, as well as the borders of the atherosclerotic carotid plaque at the far wall of the CCA. The distance for the IMT is computed between the two boundaries (at the far wall), at all points along the arterial wall segment of interest moving perpendicularly between pixel pairs, and then averaged to obtain the mean IMT ($IMT_{mean}$). The plaque is segmented at the far wall of the CCA. The near wall of the lumen was also segmented for calculating the mean lumen of D ($D_{mean}$). Also the maximum ($IMT_{max}$, $D_{max}$),

**Table 1.** Manual and Automated Mean, Maximum, Minimum And Median±(Standard Deviation) Measurements For The IMT, D, and the ICA Stenosis Performed on 20 Subjects. Values Are in [mm]. The Standard Deviations Are Given In Parentheses

| | Mean [mm] | Maximum [mm] | Minimum [mm] | Median [mm] |
|---|---|---|---|---|
| Manual Measurements | | | | |
| IMT | 0.96(0.22) | 1.14(0.37) | 0.87(0.32) | 0.95(0.33) |
| D | 5.59(0.84) | 7.43(0.89) | 3.81(0.99) | 5.45(0.91) |
| Stenosis | 48.1(11.52)% | | | |
| Automated Measurements | | | | |
| IMT | 0.93(0.25) | 1.05(0.21) | 0.81(0.25) | 0.92(0.26) |
| D | 5.77(0.99) | 7.86(1.21) | 3.75(0.66) | 6.15(1.06) |
| Stenosis | 51.05(14.51)% | | | |

IMT, D: Automated IMT and D measurements from all subjects.

**Table 2.** ROC Analysis on TPF, TNF, FPF, FNF, Overlap Index, Sp, P and F=1-E For The Atherosclerotic Carotid Plaque Snakes Segmentation Method on 20 Ultrasound Images of the CCA Bifurcation

| System Detects | Expert Detects no plaque | Expert Detects plaque | KI | Overlap Index | Sp | P | F |
|---|---|---|---|---|---|---|---|
| No plaque | TNF=98.1% | FNF=3.6% | 86% | 79.3% | 0.98 | 0.945 | 0.917 |
| Plaque | FPF=3.2% | TPF=95.2% | | | | | |

TPF, TNF, FPF, FNF: True-positive fraction, true-negative fraction, false-positive fraction, false-negative fraction, KI: Similarity kappa index, Sp: Specificity, P: Precision, F: Effectiveness measure

**Table 3.** Geometric Measurements for the Manual and the Automated Segmentation Mean±(Standard Deviation) Measurements for the CCA Bifurcation Plaque for All the 20 Ultrasound Images of the CCA. The Standard Deviations Are Given In Parentheses

| **Geometric Measures** | Manual [mm] | Automated [mm] |
|---|---|---|
| Perimeter | 50(20.66) | 48.88(20.57) |
| Area | 527.51(302) | 520.79(30.44) |
| Diameter x-axis | 22.5(9.80) | 21.66(9.62) |
| Diameter y-axis | 4.31(1.58) | 4.19(1.57) |

minimum ($IMT_{min}$, $D_{min}$ ), and median ($IMT_{median}$, $D_{median}$ ) IMT and D values, were calculated. Figure 1b illustrates the segmented $IMT_{mean}$, and $D_{mean}$ on an ultrasound image of the CCA.

### 2.6 Statistical analysis

The Wilcoxon rank sum test was used in order to identify if for each set of manual and automated segmentation measurements, a significant difference (S) or not (NS) exists between the extracted IMT, D, and plaque segmentation measurements, with a confidence level of 95%. For significant differences, we require $p<0.05$. Furthermore,

box plots for the different measurements, were plotted. Also, the correlation coefficient, ρ, between the manual and the automated measurements, which reflects the extent of a linear relationship between two data sets, was calculated. Furthermore, we estimated the true-positive fraction (TPF), true-negative fraction (TNF), false-positive fraction (FPF) and false-negative fraction (FNF) between the manual and the automated plaque segmentation measurements. We also calculated the similarity kappa index, KI, the overlap index between the manual and the automated segmentations, as well as the specificity, Sp, precision, P, and the effectiveness measure, F [15].

## 3 Results

We have evaluated in this study 20 ultrasound images of the CCA bifurcation from symptomatic subjects at risk of stroke at a mean±SD age of 48±10.47 years. Figure 1 illustrates the manual (see Fig.1a) and the automated (see Fig. 1b) IMC, plaque and D segmentation measurements performed on a normalized despeckled ultrasound image of the CCA from a symptomatic subject at the age of 53.

Figure 2 presents box plots for the mean, maximum, minimum and medina segmentation measurements of the CCA for the IMT (see Fig. 2a), and the lumen diameter, D (see Fig. 2b). From left to right, we present the mean manual and automated IMT (IMT_m, IMT), and D (D_m, D), segmentation measurements for all 20 patients investigated in this study. We observe that manual and automated segmentation measurements are very close. After performing the non-parametric Wilcoxon rank sum test, we found no statistical significant differences between the manual and the automated segmentation measurements for the IMT and the D. More specifically, we've found $p = 0.41, p = 0.86, p = 0.21$ and $p = 0.52$ for the mean, maximum, minimum and median IMT manual and automated segmentation measurements measurements, respectively. For the CCA diameter, D, we've found $p = 0.50, p = 0.52, p = 0.96$ and $p = 0.50$ for the mean, maximum, minimum and median D measurements, respectively. We finally estimated maximum ICA lumen stenosis according to (1), with (48.1±11.52)% and (51.05±14.51)% of stenosis for the manual and the automated segmentations, respectively.

Table 1 presents the manual and automated mean, maximum, minimum and mean±(Standard deviation) measurements for the IMT, D and ICA lumen stenosis performed on the 20 subjects investigated in this study.

In Table 2, we show the TPF, TNF, FPF, FNF, KI, overlap index, Sp, P, and F for the proposed snakes segmentation method, performed on all the 20 ultrasound images of the CCA bifurcation. We've found a TPF of 95.2% and an overlap index of 79.3% between the manual and the automated segmentation methods.

Finally in Table 3, we illustrate the geometric measurements for the CCA bifurcation plaque for both the manual and the automated segmentation mean±(Standard Deviation) for all the 20 images investigated.

The correlation coefficient ρ, between the mean manual and the mean automated IMT and D measurements were ρ=0.13 ($p = 0.56$) for the IMT and ρ=0.63 ($p = 0.001$) for the D, respectively.

## 4 Discussion

We proposed in this study a new snake's based segmentation system that is able to segment all three different structures of interest in an ultrasound image of the CCA, bifurcation, namely the IMC, the lumen diameter, and the atherosclerotic carotid plaque. All three different structures are important for the clinician in order to correctly evaluate the degree of the severity of the atherosclerosis disease in an asymptomatic or symptomatic individual at risk of stroke. It should be noted that this is the first automated segmentation system proposed in the literature for complete segmentation of ultrasound images of the CCA bifurcation.

The results of this study showed that there are no significant differences between the manual and the automated segmentation measurements for the IMT, lumen diameter, and the atherosclerotic carotid plaque features. The differences found between the manual and the automated segmentation measurements (see also Table 1) are in general small, as also reported in other studies for the IMT [2], [3], [16], the lumen diameter [4], [5], and the atherosclerotic carotid plaque [6]. Furthermore, the automated segmentation measurements for the IMT and the diameter, D, in this study are very close to the manual measures (see Table 1) as also reported in other studies [2]-[5]. In Table 1 we found relatively high IMT values ($IMT_{mean}$=0.96mm) and this may be attributed to the fact that the patient group was from symptomatic subjects at risk of atherosclerosis with an age of 48±10.47 years [2], [16]. It has been reported in the literature [2], [3], [11], [16] that normal IMT values lies between 0.6 mm and 0.8 mm and that symptomatic subjects at risk of atherosclerosis exhibit higher IMT values [16]. The lumen diameter, D, as well as the CSI found in this study is consistent with the normal values of the lumen diameter and stenosis found in the literature [4], [5] and it is consider to lie within the normal range of values.

From Table 2, we may also observe that the agreement between the manual and the automated plaque segmentation is very high and that the system agrees with the expert in 95% of the cases (TPF=95%) for non-detecting a plaque and 98.1% of the cases (TNF=98.1%) for detecting a plague. We can thus conclude that the automated measurements performed in this study are as much reliable and accurate as the manual measurements performed by the neurovascular expert and therefore the system may be used in the clinical praxis with confidence.

Atherosclerosis is the most common cause of stroke [5], [16]. A regular follow up is suggested for selected patients with atherosclerotic artery stenosis as well as randomized clinical trials will also be necessary to define the role and the progression of atherosclerosis in the management of these patients [5], [11], [16], [17].

The vulnerable arterial plaque may cause atherothrombotic events, myocardial infarction and stroke, which are responsible for approximately 35% of the total mortality in the western population, and are the leading causes of morbidity world-wide [17]. The first indication of CVD disease is a thickening of the intimal and medial layers of the CCA wall. It involves lipid accumulation and the migration and proliferation of many cells in the sub-intimal and medial layers, which results in the formation of plaques [16]. It is the rupture of such plaques that causes myocardial infarcts, cerebrovascular events, peripheral vascular disease and kidney infarcts. The impact of the IMT and the atherosclerotic plaques, on the incidence of CVD events in the Rotterdam study [17] using B-mode ultrasound, indicates that the risk of

myocardial infarction increases by 43% per standard deviation increase (0.163 mm) in the common carotid IMT. The main conclusions resulting from this study were supported by other independent investigations which reveal that an IMT higher than 0.9-1.0 mm [4]-[7] indicates potential atherosclerotic disease, which translates into an increased risk of a CVD event. Hence, the robust segmentation and measurement of the IMT as well as the atherosclerotic carotid plaque by B-mode ultrasound has a considerable impact in the early diagnosis of atherosclerosis, prognosis evaluation and prediction, and in the monitoring of response to lifestyle changes and to prescribed pharmacological treatments.

However, there are also some limitations for the present study, which arises mostly from the small number of subjects included and that the duration of the follow up of these patients. The study should be therefore, further applied on a larger sample of subjects, a task which is currently undertaken by our group. Additional variables, such as age, sex, weight, blood pressure and other atherosclerotic risk factors should be taken into account for better evaluating the atherosclerotic process and disease and the risk of stroke in this group of patients.

## 5 Concluding Remarks

In this paper we present a new snakes based segmentation system for the complete segmentation of the CCA bifurcation in ultrasound images. It should be noted that this is the first semi-automated integrated segmentation system proposed in the literature for the complete segmentation of the CCA. We anticipate in the future to apply the proposed system in a larger group of subjects and to extract texture characteristics from the segmented areas (IMC and carotid plague). These texture characteristics can then be used to classify and or separate subjects with increased IMC structures, as it was shown in [18], in different risk groups. Additionally, features extracted from the atherosclerotic carotid plaque, may be used for the separation between asymptomatic and symptomatic subjects. However, a larger scale study is required for evaluating the system before its application in the real praxis.

## References


1. Mendis, S., Puska, P., Norrving, B.: Global Atlas on cardiovascular disease prevention and control. WHO (2012) ISBN: 978-92-4-156437-3
2. Molinari, F., Zeng, G., Suri, J.S.: A state of the art review on intima-media thickness measurement and wall segmentation techniques for carotid ultrasound. Comp. Meth. and Progr. in Biomed. 100, 201--221 (2010)
3. Loizou, C.P., Pattichis, C.S, Pantziaris, M., Tyllis, T., Nicolaides, A.N.: Snakes based segmentation of the common carotid artery intima media. Med. Biolog. Eng. Comput. 45, 35--49 (2007)
4. Bladin, C.F., Alexandrov, A.V., Murphy, J., Maggisano, R., Norris, J.W.: Carotid Stenosis Index. A New Method of Measuring Internal Carotid Artery Stenosis. Stroke 26, 230--234 (1995)

5. Eigenbrodt, M. L., Sukhija, R., Rose, K. M., Tracy, R.E., et al.: Common carotid artery wall thickness and external diameter as predictors of prevalent and incident cardiac events in a large population study. Cardiovascular Ultrasound 5, 11, 1--11 (2007)
6. Loizou, C.P., Pattichis, C.S., Pantziaris, M., Nicolaides, A.N.: An integrated system for the segmentation of atherosclerotic carotid plaque. IEEE Trans. Inform. Techn. Biomed. 11, 6, 661--667 (2007)
7. Loizou, C.P., Pattichis, C.S., Nicolaides, A.N., Pantziaris, M.: Manual and automated media and intima thickness measurements of the common carotid artery. IEEE Trans. Ultras. Ferroel. Freq. Contr. 56, 5, 983--994 (2009)
8. Loizou, C.P., Pattichis, C.S.: Despeckle filtering algorithms and Software for Ultrasound Imaging. Synthesis Lectures on Algorithms and Software for Engineering, Ed. Morgan & Claypool Publishers, 1537 Fourth Street, Suite 228, San Rafael, CA 94901 USA (2008)
9. Loizou, C.P., Pattichis, C.S., Christodoulou, C.I., Istepanian, R.S.H., Pantziaris, M., Nicolaides A.: Comparative evaluation of despeckle filtering in ultrasound imaging of the carotid artery. IEEE Trans. Ultras. Ferroel. Freq. Contr. 52, 10, 1653--1669 (2005)
10. A Philips Medical System Company. Comparison of image clarity, SonoCT real-time compound imaging versus conventional 2D ultrasound imaging. ATL Ultrasound, Report (2001)
11. Elatrozy, T., Nicolaides, A.N., Tegos, T., Zarka, A., Griffin, M., Sabetai, M.: The effect of B-mode ultrasonic image standardization of the echodensity of symptomatic and asymptomatic carotid bifurcation plaque. Int. Angiol. 17, 3, 179--186 (1998)
12. North American Symptomatic Carotid Endarterectomy Trial Collaborators: Beneficial effect of carotid endarterectomy in symptomatic patients with high-grade carotid stenosis. N. Engl. J. Med. 325, 445--53 (1991)
13. Lee, J.S.: Refined filtering of image noise using local statistics. Comp. Graph. and Image Process. 15, 380--389 (1981)
14. Williams, D.J., Shah, M.: A fast algorithm for active contours and curvature estimation. Int. J. on Graph., Vision and Imag. Proc.: Image Underst. 55, 14--26 (1992)
15. Metz, C.: Basic principles of ROC analysis. Semin. Nucl. Medic. 8, 283--298 (1978)
16. Bots, M.L., Hofma, A., Diederick, E. G.: Increased common carotid Intima-media thickness. Adaptive response or a reflection of atherosclerosis? Findings from the Rotterdam Study. Stroke 28, 2442--2447 (1997)
17. van der Meer I. M., Bots M. L., Hofman A., del Sol A. I., van der Kuip D. A., Witteman J. C.: Predictive value of noninvasive measures of atherosclerosis for incident myocardial infarction: The Rotterdam Study. Circulation 109, 9, 1089--1094 (2004)
18. Loizou, C.P., Pantziaris, M., Pattichis, M.S., Kyriakou, E., Pattichis, C.S.: Ultrasound image texture analysis of the intima and media layers of the common carotid artery and its correlation with age and gender. Comput. Med. Imag. Graph. 33, 4, 317--324 (2009)